VOLUME 76 SEPARATE No. 24

Illinois U Library

ROCEEDINGS

AMERICAN SOCIETY OF CIVIL ENGINEERS

JUNE, 1950

BUCKLING OF RIGID-JOINTED PLANE TRUSSES

By N. S. Hoff, Bruno A. Boley, S. V. Nardo, and Sara Kaufman

STRUCTURAL DIVISION

Headquarters of the Society
33 W. 39th St.
New York 18, N.Y.

PRICE $0.50 PER COPY

The Society is not responsible for any statement made or opinion expressed in its publications

Published at Prince and Lemon Streets, Lancaster, Pa., by the American Society o
Civil Engineers. Editorial and General Offices at 33 West Thirty-ninth Street,
New York 18, N. Y. Reprints from this publication may be made on
condition that the full title of paper, name of author, page
reference, and date of publication by the Society are given.

***Copyright 1950 by the* AMERICAN SOCIETY OF CIVIL ENGINEERS**

Printed in the United States of America

AMERICAN SOCIETY OF CIVIL ENGINEERS
Founded November 5, 1852
PAPERS

BUCKLING OF RIGID-JOINTED PLANE TRUSSES

By N. J. Hoff,[1] Bruno A. Boley,[2] S. V. Nardo,[3]
and Sara Kaufman[4]

Synopsis

The buckling loads of two welded and six riveted frameworks were calculated by the convergence criterion of the method introduced by Hardy Cross, Hon. M. ASCE. The stiffening effect of the gusset plates was taken into account and the reduction in the effective modulus caused by stresses exceeding the elastic limit was considered. Values of stiffness coefficients and of carry-over factors are presented in graphs for bars with gusset plates of various length. Tests of eight frameworks are described and the experimental buckling loads are compared with those calculated from the theory. Good agreement was obtained for frameworks buckling in the elastic range.

When the stresses exceeded the elastic limit, the choice of the correct value of the effective modulus presented a problem because large bending moments were observed in the bars before they buckled. These moments seemed to depend on the initial curvature and eccentricity of the bars and their magnitude could not be predicted theoretically. On the other hand, they influenced the effective modulus. In spite of the uncertainties involved in the choice of the effective modulus, reasonable agreement between theory and experiment was found with frameworks buckling in the inelastic range. Nevertheless, further investigation of this problem is indicated.

Introduction

The braced framework is one of the oldest types of structures and its analysis has been developed through centuries. However, comparatively little effort has been made to calculate its failing load accurately. If the framework

---

Note.—Written comments are invited for publication; the last discussion should be submitted by **December 1, 1950.**

[1] Prof. of Aeronautical Eng., Polytechnic Inst. of Brooklyn, Brooklyn, N. Y.

[2] Asst. Prof. of Aeronautical Eng., Polytechnic Inst. of Brooklyn, Brooklyn, N. Y.

[3] Instr. in Aeronautical Eng., Polytechnic Inst. of Brooklyn, Brooklyn, N. Y.

[4] Research Asst., Polytechnic Inst. of Brooklyn, Brooklyn, N. Y.

fails through rupture of the material in one of the members, the maximum load the structure can sustain may be calculated simply as the load at which the stress somewhere in the framework first reaches its ultimate value. However, if the bars of the framework are slender, failure is more likely to occur through buckling and the foregoing method of computing the maximum load is no longer applicable. It has been customary, in the determination of the buckling load of frameworks, to examine each bar individually and to calculate the buckling load by the Euler formula or by some short column formula. These calculations always involve an assumption of the value of the end fixity coefficient or of the effective length of the framework member.

In reality if any one bar in a rigid-jointed framework buckles, the rigidity of the joints implies that at the same time all the bars riveted to the ends of the first bar must distort. Since these adjacent bars are rigidly attached to other bars of the framework, a continuation of the reasoning shows that in the buckling of any one bar all the bars of the framework must be involved. The buckling load of a framework depends, therefore, not only on the mechanical and geometric characteristics of the highly compressed member but also on the amount of end restraint offered to this member by adjacent bars whose stiffnesses in turn are influenced by the stiffnesses of their neighbors. Depending on the amount of end restraint, the end fixity coefficient of a perfectly elastic bar varies from 1 to 4, corresponding to zero and infinite resistance to rotation of the ends of the member. As it is impossible to estimate correctly the actual amount of restraint, the method of calculating the buckling load of a framework by analyzing each bar individually leads to unreliable results.

An additional complication arises from the fact that the stiffness, or resistance to rotation, of a bar depends upon the load the bar is carrying. For instance, a tension member attached to the end of a compression member stiffens the latter, and this effect increases if the tensile load becomes higher. Thus the buckling load of the most highly compressed bar of a framework is influenced by the forces to which each member of the rigid-jointed framework is subjected.

The interaction of all these effects can be taken into account simultaneously if the buckling load of the framework is calculated by the convergence criterion of the Hardy Cross method. The criterion was proved by one of the writers (Mr. Hoff)[5,6,7] in various articles and in an address before the Second Annual Meeting of the Institute of the Aeronautical Sciences at Pasadena, Calif., on June 24, 1940. The purpose of this paper is an experimental verification of the theory and the development and presentation of stiffness coefficients and carry-over factors for bars whose ends are reinforced by gusset plates. In addition, the effects of stresses exceeding the elastic limit, of initial eccentricities and curvature, and of joint displacements are investigated.

THE CONVERGENCE CRITERION

The Hardy Cross Moment Distribution Method.—The rigid-jointed braced framework of Fig. 1 is supported in a statically determinate manner. If a

---

[5] "Stable and Unstable Equilibrium of Plane Frameworks," by N. J. Hoff, *Journal of the Aeronautical Sciences*, January, 1941, p. 115.

[6] "The Proportioning of Aircraft Frameworks," by N. J. Hoff, *ibid.*, June, 1941, p. 319.

[7] "Stress Analysis of Aircraft Frameworks," by N. J. Hoff, *Journal of the Royal Aeronautical Society*, Vol. XLV, 1941, p. 241.

moment M acting in the plane of the truss is applied to one of the joints, for instance, to joint A, the joint rotates and the applied moment is distributed among the bars attached to the joint. Equilibrium of the truss requires that the moment be balanced by reactions at the points of attachment of the cantilever truss to the rigid wall. It can be shown that the axial loads caused in the various bars by the moment and its reactions are negligibly small because the bending rigidities of the individual bars are small as compared to the bending rigidity of the entire truss. Similarly, the linear displacements of the joints due to the moment and its reactions at the wall can be safely neglected.

Consequently, the framework of Fig. 1 can be analyzed as a problem in moment distribution disregarding the forces that are required at the joints to establish equilibrium. Analysis by the Hardy Cross moment distribution method involves a balancing moment distributed among the bars joined at point A in the ratio of their stiffnesses. The stiffnesses are calculated on the assumption that the far ends of the bars (at joints B, C, D, E, and F) are rigidly fixed against rotation (see Appendix 1). The moment required for fixing the far end is known as the carry-over moment. It is the product of the moment that became the share of any one bar in the balancing process and the carry-over factor of the same bar. The carry-over moment at any one of the joints B, C, D, E, or F is then considered as the unbalanced moment and is balanced. The balancing moments are distributed, the carry-over moments calculated, and the various steps of the procedure repeated at all the joints until the unbalanced moments that remain are considered negligibly small. The unbalances can always be made arbitrarily small if a sufficiently large number of suitable individual steps is undertaken. Moreover, it is always easy to find a suitable sequence of operations. One such sequence is established, for instance, by the rule that in each step the largest unbalanced moment should be balanced.

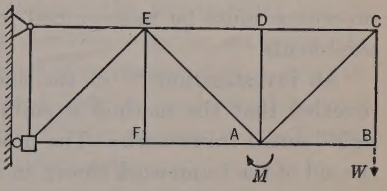

FIG. 1.—FRAMEWORK AND LOADS

Convergence of the Procedure.—A process in which the unbalanced moments can be reduced at will is known as a convergent process. The resultant bending moments at the ends of the bars converge to (that is, approach) finite values which are identical with those that can be obtained from an analytical solution of the moment distribution problem. The Hardy Cross process converges since the share of each bar after each distribution is smaller than the original unbalanced moment at the joint; and the carry-over factor is $\frac{1}{2}$ for bars of constant moment of inertia as long as the effect of the axial forces in the bars is neglected.

The situation is more complex when the individual bars of the framework are under the action of axial forces. Such axial forces can be caused, for instance, by a vertical downward load W applied to joint B. It is known that they can be calculated with sufficient accuracy by assuming ideal pin joints at the junctures of the bars even though in reality the bars are connected by sturdy gusset plates. The effect of the axial forces on the stiffness coefficients and the carry-over factors, however, should not be neglected. Values of these quantities have been calculated and presented in graphs and tables by Benjamin Wiley James[8] and A. S. Niles,[9] Assoc. M. ASCE, as well as by Eugene E. Lundquist, Assoc. M. ASCE, and W. D. Kroll[10] for different values of the governing parameter L/j, in which L is the geometric length of the bar, and j is defined by

$$j = \sqrt{\frac{E\,I}{P}} \qquad (1)$$

In Eq. 1 the product $E\,I$ is the bending rigidity of the bar and P is the absolute value of the axial force acting upon it. Since in these tables the stiffness factor has negative as well as positive values and the carry-over factor is often much greater than unity, the question of the convergence of the Hardy Cross procedure must be re-examined for the case when the bars are subjected to axial loads.

An investigation[5,6,7] of the convergence of the Hardy Cross method has revealed that the method is suitable for establishing the stability limit of a rigid-jointed framework. The procedure recommended can be explained with the aid of the framework shown in Fig. 1. It is assumed that the only external load is a vertical downward force W at joint B. When the force W is small, obviously the structure is stable; and, when the force is increased, a value is eventually reached at which the framework buckles. The problem is to calculate this critical value of the applied load.

Calculation of the Buckling Load.—The first step in the calculation is the determination of the axial loads in all the bars of the framework corresponding to an assumed value of the external load W. Next the $\frac{L}{j}$-ratios are computed for each bar. When the $\frac{L}{j}$-values are smaller than π in all the compression bars, the framework is stable because each of its bars would be stable even if the bars were attached to one another by ideal pin joints. When $\frac{L}{j}$ is greater than $2\,\pi$ in any one compression bar, the entire truss is unstable because the bar in question would be unstable even if its two ends were rigidly fixed. When some of the $\frac{L}{j}$-ratios are greater than π but none of them is greater than $2\,\pi$, further calculations are necessary to determine stability.

In such a case the stiffness coefficients have to be taken from the tables or graphs and the stiffnesses S must be calculated for each bar. The stiffness S

---

[8] "Principal Effects of Axial Load on Moment-Distribution Analysis of Rigid Structures," by Benjamin Wiley James, *Technical Note No. 534*, National Advisory Committee for Aeronautics, Washington, D. C., July, 1935.

[9] "Airplane Structures," by A. S. Niles and J. S. Newell, John Wiley & Sons, Inc., New York, N. Y., 3d Ed., 1943, Vol. 2, p. 121.

[10] "Tables of Stiffness and Carry-Over Factors for Structural Members Under Axial Load," by Eugene E. Lundquist and W. D. Kroll, *Technical Note No. 652*, National Advisory Committee for Aeronautics, Washington, D. C., June, 1938.

is defined as $\frac{L}{EI}$ multiplied by the stiffness coefficient. The sums of the stiffnesses must be positive at each joint. If at any one joint the sum ΣS is zero or negative, the subsystem comprising that particular joint and all the bars attached to it would be unstable even if the far ends of the bars were all rigidly fixed. Hence, the entire framework would also be unstable.

The conditions on $\frac{L}{j}$ and ΣS establish upper and lower limits for the critical value of the applied load. The condition on ΣS is correct for bars with or without gusset plates but the limits π and 2π stated for $\frac{L}{j}$ are increased by the gusset plate effect. The increases are moderate for frameworks of customary design. Use of the foregoing limits leads to conservative design when the bars have gusset plates. Within the upper and lower limits the stability can be checked by the convergence criterion. The criterion may be stated in the following form: Convergence to a finite unique set of end moments in a straightforward application of the Hardy Cross moment distribution method is proof of the stability of the framework provided the stiffness and carry-over factors are determined with due consideration of the axial loads.

The convergence can be checked by assuming a moment of arbitrary magnitude at any one of the joints—for instance at point A in Fig. 1. With the aid of the stiffness and carry-over factors corresponding to the chosen value of W, a routine moment distribution is carried out. If the calculator succeeds in "whittling down" the unbalanced moments to negligibly small quantities at all the joints, the procedure converges and by the convergence criterion the framework is stable. Next a larger value of W is selected and the $\frac{L}{j}$-values and ΣS-values are computed. If the procedure again converges, a still larger value of W is chosen until it is found that the unbalanced moments increase rather than decrease after a number of balancing operations. Then it is known that the framework is unstable under the chosen load W.

Theoretically, the lack of convergence can be caused either by actual instability of the framework or by the incompetence of the calculator. However, experience has shown that the average engineer conversant with the moment distribution method has no difficulty in converging the process when the applied load is 1% or 2% smaller than the theoretical critical load. Similarly, the divergence is very marked as soon as the applied load exceeds the critical value by 1% or 2%. Consequently, the buckling load can be bracketed very closely with little effort if the convergence criterion is used. It is immaterial to which joint the moment M is applied but experience has shown that the convergence, or its absence, can be judged with the least effort if the moment is assumed to act at the joint to which the most highly compressed bars are attached. Details of the calculations are evident from the example presented in Appendix 2.

Proof of the Convergence Criterion.—The proof of the convergence criterion was published in various places during 1941.[5,6,7] It is based on properties of the total potential of the system which is the sum of the strain energy stored in the framework and the potential of the external loads. It can be shown that the analytical expression for the total potential of a stable framework has a minimum value with respect to the rotations of all the joints when the framework is in equilibrium. Each cycle of the moment distribution procedure consisting of balancing, distributing, and carry-over corresponds to a rotation of the joint balanced. The angle of rotation is of the magnitude required for the equilibrium of the subsystem comprising the joint and the bars attached to it. As in each step of the moment distribution procedure the far ends of the bars are considered rigidly fixed, the subsystem is always stable because of the requirement $\Sigma S > 0$. Consequently, the establishment of equilibrium in the subsystem decreases the total potential of the subsystem to its minimum (compatible with the requirement of no rotations at the far ends of the bars) and diminishes the value of the total potential of the entire framework.

It is known, therefore, that in each cycle of the balancing procedure the total potential of the system decreases and thus approaches the minimum corresponding to stable equilibrium. At the same time the moments at the ends of the bars approach the values that prevail when the system is in equilibrium. Experience with numerical examples has shown that the approach is quite rapid or, in other words, that the procedure is well convergent.

On the other hand, when the framework is unstable under the loading, equilibrium corresponds to either a maximum or a saddle point of the total potential of the system. Consequently, the moment distribution procedure whose every step diminishes the total potential cannot lead, as a rule, to the unstable state of equilibrium, and the end moments cannot approach values that correspond to equilibrium. After a limited number of initial cycles the difference between the instantaneous value of the total potential and the value corresponding to unstable equilibrium becomes greater in each cycle of the moment distribution process, and the unbalanced moments increase rather than decrease. Therefore, the moment distribution process is divergent.

Theoretical examples illustrating the different behavior patterns have been presented elsewhere[7] and the changes in the values of the total potential during the individual steps of the moment distribution process were plotted in diagrams. It was also shown that for particular types of loading certain sequences in the balancing procedure may lead to equilibrium even though the system is unstable. In such cases, however, any change in the sequence causes a divergence of the process and thus the set of end moments obtained is not unique. In practical analysis such an occurrence is most unlikely.

Extension of the Original Theory.—As the convergence criterion is based on theorems well established in mechanics, an experimental verification of the criterion proper is not required. Nevertheless, eight specimens were constructed and tested in the aeronautical laboratories of the Polytechnic Institute of Brooklyn at Brooklyn, N. Y., mainly for the following reasons: In the basic theory each bar is replaced by a mathematical line segment, the center line of the bar, ending at the intersection points of the center lines, and the bending rigidity of the bar is considered constant. In reality the bars have finite cross-sectional dimensions, and they are attached to one another by rigid gusset plates. Consequently, in the vicinity of the joints the bars are stiffened by the gusset plates and by the other bars converging in the same joint, with the result that the bending rigidity of the ends is greater than that of the middle of the bar. The effect of this increase in bending rigidity is an increase in the buckling load of the framework which can be considerable when the gusset plates are large. The problem is amenable to a theoretical solution after suitable assumptions are made for the variation of the bending rigidity of the bar in the region where it is reinforced by the gusset plate. The validity of the assumptions can only be checked by experiments. Moreover, tests are required to obtain information regarding reduced modulus values when the stresses in some bars exceed the elastic limit of the material before the framework buckles.

Gusset Plate Effects.—Both bending and buckling tests showed conclusively that actual bars with gusset plates are considerably stiffer then their theoretical counterparts which are assumed to have a constant rigidity between their mathematical end points. The rather obvious next assumption is to consider the bending rigidity constant from gusset plate to gusset plate and infinitely large between the edge of the gusset plate and the mathematical end point of the bar. However, experiments indicate that this assumption makes the bars materially stiffer than they are in reality. Therefore, a further refinement in the assumption is necessary. Each bar is considered to have its actual constant bending rigidity between the gusset plates, and this rigidity is increased according to a hyperbolic law from the edge of the gusset plate to the mathematical end point of the bar where the rigidity becomes infinite. This assumption gave satisfactory agreement with bending and buckling tests when the gusset plates were not excessively large. When their length amounted to 16% or 20% of the length of the bar, the hyperbolic law gave too conservative results. In almost all cases the experimental points fell between the theoretical results calculated from the infinite gusset plate rigidity and the hyperbolic law assumptions.

Values of the stiffness factors have been computed[11] for both the infinite rigidity and the hyperbolic law assumptions for bars not subjected to axial loads. In Appendix 1, these calculations are extended to bars with compressive or tensile end loads. At the same time values of the carry-over factor are also determined. The numerical values computed are presented in a number of diagrams.

Inelastic Buckling.—Although the gusset plate problem can be considered as solved satisfactorily for practical purposes, efforts made to establish rules for the determination of effective modulus values, when the stresses in the framework exceed the elastic limit, could not be brought to a final conclusion. It was observed in the tests that the bars of the framework were subjected to considerable bending moments and were visibly curved before the framework buckled. Thus, bending stresses were superimposed upon the uniformly distributed compressive stresses in the bars.

---

[11] "Transversely Loaded Framework Members," by N. J. Hoff, *Journal of the Royal Aeronautical Society*, Vol. XXXIX, 1935, p. 718.

A diagram was developed on the assumption of the constancy of the axial load which permits an easy determination of the reduced modulus when the extreme fiber strains are known. The difficulty lies in finding the extreme fiber strains. An attempt was made in this investigation to explain the bending moments in the bars by calculating the secondary stresses and evaluating the effects of initial curvature and eccentricity.[12] It was found possible to assume curvature and eccentricity values which yielded extreme fiber strains in satisfactory agreement with those measured in the different stages of loading, but no method of predicting such values in a new design could be found. Moreover, the assumption of a constant compressive force during the buckling process is open to question in view of the work reported by F. R. Shanley.[13,14]

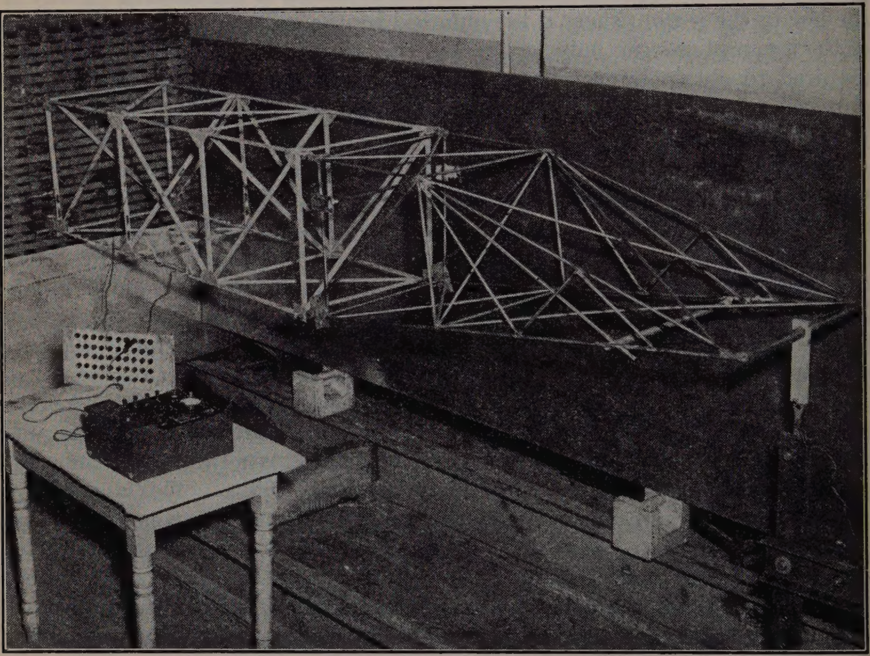

FIG. 2.—TEST SPECIMEN AND RIG

The final solution of the buckling problem of frameworks in the inelastic range cannot be expected until the basic problem of the inelastic buckling of columns is clarified completely. On the other hand, this clarification would be accelerated if more experimental data were obtained in tests on rigid-jointed frameworks.

---

[12] "Buckling of Rigid-Jointed Frameworks," submitted by Dept. of Aeronautical Eng. and Applied Mechanics of the Polytechnic Inst. of Brooklyn, Brooklyn, N. Y., to the Office of Naval Research of the U. S. Navy under contract N6onr-263, Task Order I, Washington, D. C., February, 1948.

[13] "The Column Paradox," by F. R. Shanley, *Journal of the Aeronautical Sciences*, December, 1946, p. 678.

[14] "Inelastic Column Theory," by F. R. Shanley, *ibid.*, May, 1947, p. 261.

DESCRIPTION OF EXPERIMENTS AND COMPARISON OF TEST RESULTS WITH THEORY

Test Specimens.—Eight framework specimens were tested in the course of this investigation. Of these all but one failed through buckling; of the seven that buckled two were designed to fail in the inelastic range and the other five buckled with stresses below the proportional limit.

A specimen and the test setup are shown in Fig. 2. Each framework was made of two identical vertical planes with a length-to-height ratio of 3:1, these two planes being connected by horizontal and diagonal braces so as to constitute a three-dimensional framework. Such a construction was considered necessary to avoid buckling out of the plane in the framework. However, in the analysis the stiffening effect of the braces between the two planes was neglected so that the frameworks were in effect considered to be two dimensional.

The configuration of the vertical planes of each framework is shown in Fig. 3. The frameworks were tested under the combined action of a vertical load and a bending moment applied in such a way as to cause tension in the upper chords and compression in the lower chords.

Specimens 1 and 2 were of welded steel construction, and the remaining six specimens were riveted of 24S-T aluminum alloy. The gusset plate length was measured from the center of the joint to the center of the outermost rivet. Rounded out values of these lengths are indicated in Fig. 3. Specimen 5 (Fig. 3(*d*)) was tested twice, first with the last rivets missing so that the effective gusset plate length was about 13% of the length of the bar and then with all rivets driven and thus with a gusset plate length of approximately 20% of the length of the bar. This procedure was possible because the deformations under the buckling load were fully elastic with specimens 1 to 5. Specimens 6 to 8 failed at stresses exceeding the elastic limit.

Test Rig and Test Procedure.—The specimens were connected to the rigid wall of the test rig which accommodated a fitting to which the specimen was pinned at its upper end. The lower end of the specimen was fitted with either a roller bearing or a bushing which bore against a smooth plate fastened to the rig. The specimens were loaded in cantilever fashion through a loading frame attached to the specimen itself by pins, so that no bending moment could be transmitted at the joint. The point of the application of the load was always at a distance from the rigid wall equal to twice the length of the specimen. The load was applied to the loading frame by a mechanical jack and lever arrangement, and was measured by a pair of SR-4 type A-1 "metalectric" strain gages cemented to opposite sides of a calibrated load link.

The strains in some of the members of the framework specimens were determined with the aid of SR-4 type A-1 or A-11 "metalectric" strain gages. Usually the gages were cemented at any one location in pairs, on opposite sides of the framework member. This arrangement allowed the measurement of the pure axial strain directly when the pairs of gages were connected in series, or of the bending moment when they were connected in parallel. For some of the specimens, however, individual strain measurements were recorded.

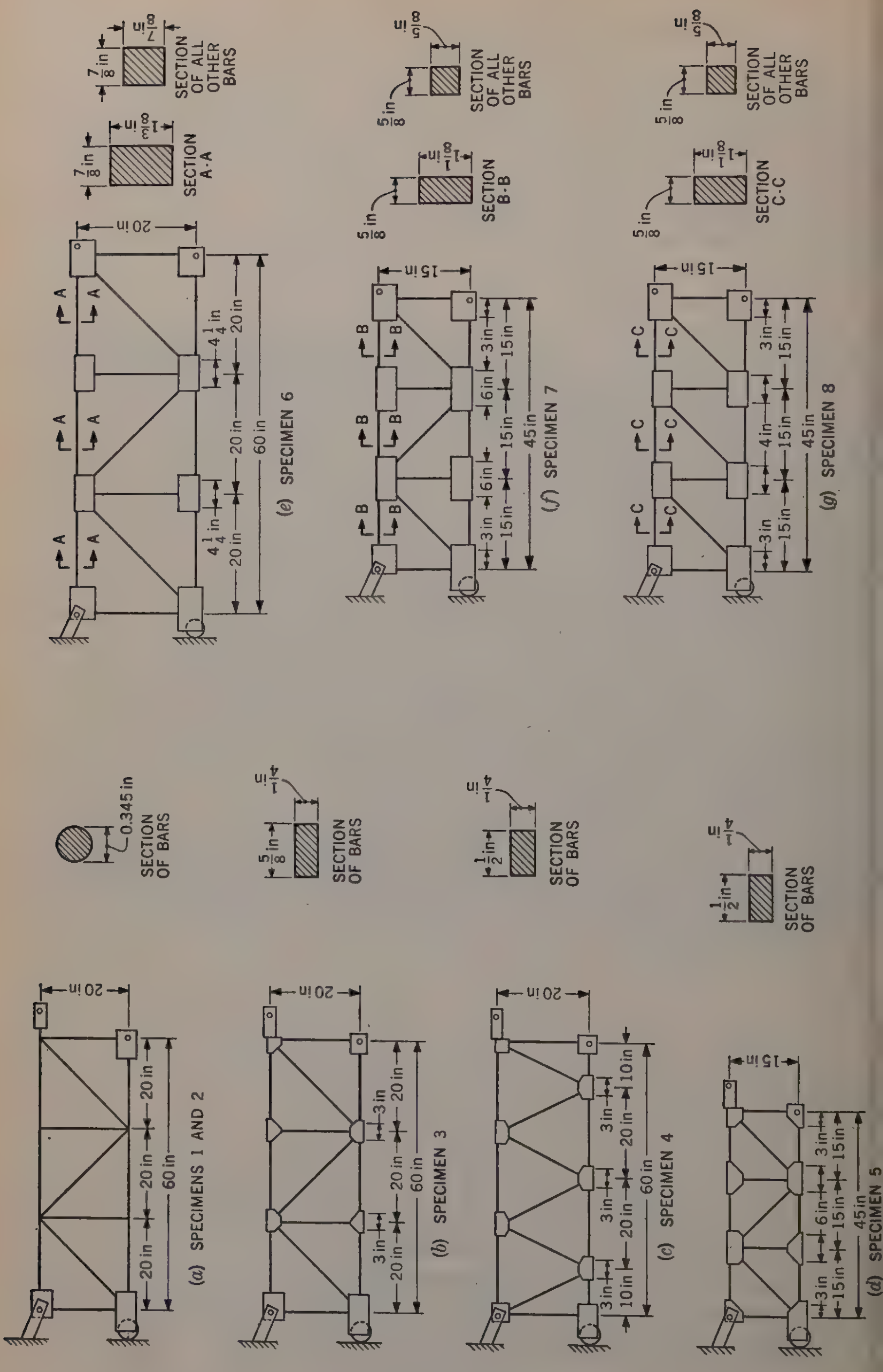

(a) SPECIMENS 1 AND 2

(b) SPECIMEN 3

(c) SPECIMEN 4

(d) SPECIMEN 5

(e) SPECIMEN 6

(f) SPECIMEN 7

(g) SPECIMEN 8

The strain was measured with an SR-4 portable electronic strain indicator. Switching from one strain gage to another was accomplished by a banana plug and jack arrangement. The load link was calibrated in a lever-type testing machine.

The test procedure adhered approximately to the following outline: For four or five values of the load below the critical value, force and bending moment data were recorded for the framework members equipped with gages. The load was then slowly increased to the buckling or critical value while simultaneous strain readings were taken on gages on the upper and lower side of the most highly compressed bar. Thus, the strains in this bar were known to the moment of buckling. They were needed in the calculation of the reduced modulus.

With specimens failing in the elastic or Euler range the buckling load was observed as the load at which a continued deflection of the point of application of the load was noted without an increase in the load. With specimens failing in the inelastic range the value of the load dropped suddenly when the framework buckled.

Care was taken that the shear and bending moment be evenly applied to the two panels of the framework. Equalization of the load was attained by placing shims under the roller bearings or by shifting the point of application of the load.

Comparison of Calculated and Measured Buckling Loads

It was mentioned that in the calculations the actual framework was replaced by its two vertical plane trusses. Consequently, the stiffening effect of the braces connecting the two vertical planes of the actual framework was entirely neglected. It is believed that the buckling loads of the frameworks were not materially influenced by the stiffness of these braces because an effort was made to have the applied load equally distributed between the two vertical planes of the framework. The displacement patterns of the two vertical planes were always very similar, and thus the motion of the braces connecting the two planes consisted mainly of a rigid body motion with little twisting or bending. A check on the additional stiffness provided by the braces was made in the experiments in which the theory of gusset plate stiffness was verified. The assumption that the braces are not of major importance was substantiated by these tests.

The experimental buckling loads are presented in Table 1 together with the nominal values of the gusset plate size. Table 1 also contains the calculated buckling loads with the effect of the gusset plates neglected, with a hyperbolic variation of the bending rigidity in the gusset plate regions, and with an infinite moment of inertia in these regions. Where appropriate, the effective modulus of elasticity was taken into account.

With frameworks 1 to 5 (Fig. 3), which buckled elastically, the buckling load obtained with the effect of the gusset plate neglected is always lower than the corresponding experimental load. (It should be noted that specimens 1 and 2 (Fig. 3(*a*)) had gusset plates only on one bar at one joint.) When the hyperbolic variation of bending rigidity is assumed, the agreement between experimental and theoretical loads is materially improved, the largest percentage error being (with one exception) 5% as compared to 18.3% obtained when the gusset plates were neglected. (All percentages are based on the experimental values.) The one exception is the test run on specimen 5 with gusset plates extending over 20% of the length of the members. In this case the errors are 44.7% and 27.7% when the gusset plates are neglected and considered, respectively. The conclusion is then reached that the assumption of a hyperbolic variation is not sufficiently accurate for bars with gusset plates whose length is of the order of magnitude of 20% of the length of the bar, but represents with a satisfactory degree of accuracy the behavior of bars with gusset plates extending over not more than about 13% of the length. Furthermore, with the exception of specimen 1 which showed a difference of only 1.1% between theory and experiment, all values calculated from the hyperbolic variation assumption are slightly lower than the actual buckling load and are, therefore, conservative.

TABLE 1.—BUCKLING LOADS OF TEST SPECIMENS

Specimen No. (see Fig. 3)	Nominal gusset plate size[a]	COMPUTED BUCKLING LOADS				Experimental buckling loads	ERROR BASED ON EXPERIMENTAL VALUE (%)			
(1)	(2)	Gussets neglected (3)	Variable rigidity (4)	Infinite rigidity (5)	Reduced modulus[b] (6)	(7)	Gussets neglected (8)	Variable rigidity (9)	Infinite rigidity (10)	Reduced modulus[b] (11)
1	12[c]	407	440	....	....	435	− 6.4	+ 1.1	....	....
2	12[c]	407	440	....	....	445	− 8.5	− 1.1	....	....
3	9	178	178	225	....	184	− 3.2	− 3.2	+21.2	....
4	9	175	205	255	....	216	−18.0	− 5.1	+18.1	....
5	13	245	300	360	....	300	−18.3	0	+20.0	....
5	20	245	320	520	....	443	−44.7	−22.7	+17.3	....
6	10	10,520	....[d]	....[d]	....[d]	....	....	....	....	....
7	20	4,950	6,300	....	5,875	5,600	−11	+12.5	....	+4.9
8	15	5,750	....	....	5,875	5,420	....	....	....	+8.4

[a] Percentage of bar length. [b] Reduced modulus and variable rigidities. [c] Gusset plate only at roller bearing. [d] Did not fail by buckling.

As the upper limit for the stiffness is represented by the assumption of an infinite moment of inertia in the regions of the gusset plates, the buckling loads were next calculated on this basis. The results obtained were always substantially higher than the experimental values, as may be seen from Table 1. Consequently, the buckling loads calculated from the assumption of an infinite rigidity must be considered unsafe.

Specimen 6 (Fig. 3(*e*)) did not fail by buckling but by the shearing of some of the riveted connections. The stresses at failure in the most highly compressed member of specimen 7 were above the proportional limit of the material. For this reason a reduced modulus of elasticity E_r was used in the calculations. Since E_r depends on the strains at the two extreme fibers at the bar, care was taken in the experiment to measure the strains in the highly loaded bars at sufficiently close intervals to allow an extrapolation to the moment of failure. The strains were found to vary somewhat along the bars. The stiffness and carry-over factors were calculated with the aid of a single value for the modulus of elasticity for any particular bar, and thus it was necessary to replace the variable modulus distribution along the bar by a constant value. In obtaining this average modulus more weight was given to the values along the middle of the bar. Table 1 shows that the buckling load calculated with consideration of the effects of both the reduced modulus and the gusset plates is in satisfactory agreement with experiment.

Specimen 8 was the second framework designed to fail in the inelastic range. The critical load calculated for this specimen by the convergence criterion, neglecting the effects of the gusset plates and of the stresses above the proportional limit was 5,750 lb, applied at the end of the loading frame. It was not expected that the experimental buckling load would differ materially from this value; yet, when the load of 4,600 lb was reached in the test, one of the vertical bars of the specimen suddenly appeared to undergo a vertical translation and possibly also some stretching. The value of the applied load dropped and the zero positions of the strain gages were altered so much that no reliable strain readings could be obtained afterward. It was possible, however, to increase the applied load to a value of 5,420 lb, at which time the framework failed in the more usual displacement pattern involving only rotations of the joints. No further increase in the load was possible.

Because strain readings were not available near the maximum load, the effective modulus could not be calculated with any degree of accuracy. When the effective modulus corresponding to the average compressive stress was computed from the von Kármán expression and the gusset plate effect was neglected, the buckling load of the framework was found to be 5,400 lb by the convergence criterion. The buckling load was also calculated on the assumption of a hyperbolic increase of the stiffness in the gusset plate region. At the same time the modulus was taken equal to the tangent modulus corresponding to an average compressive stress calculated for a pin-jointed framework. The load obtained was approximately 5,875 lb and therefore did not differ widely from the experimental value. In view of the uncertainties involved in the choice of the effective modulus the agreement obtained between theory and experiment can be considered satisfactory provided the final experimental buckling load is considered as the correct one.

Joint Displacements.—In an attempt to obtain an explanation for the sudden change in the displacement pattern of specimen 8 at the lower load of 4,600 lbs, the buckling load of this framework was also evaluated considering the displacements as well as the rotations of the joints. In the calculations the Hardy Cross method had to be replaced by the more general Southwell approach and the technique employed was that suggested by one of the authors (Mr. Boley[15]). When the only displacements taken into account were those of the joints at the ends of the vertical bar which underwent a translation, the value obtained for the load was 5,400 lb which was practically indistinguishable from that given by the Hardy Cross method. When the displacements of all the joints were considered, the buckling load was found to be between 5,340 lb and 5,400 lb, thus showing only a negligible change in the value of the buckling load. Both calculations including joint displacements were carried out on the basis of a value of the reduced modulus of elasticity calculated from the von Kármán formula. It was concluded that the unusual behavior of the framework was not due to buckling involving joint displacements, but was probably due to some inaccuracy in the construction or test setup. Unfortunately, because of lack of time this conclusion could not be checked experimentally by testing a second specimen of the same design.

---

[15] "Numerical Methods for the Calculation of Elastic Instability," by Bruno A. Boley. *Journal of the Aeronautical Sciences*, June, 1947, p. 337.

A systematic, although somewhat limited, theoretical investigation of the effect of joint displacements on the instability of rigid-jointed frameworks led to the conclusion that this effect is negligible.

Stiffness Tests.—The correctness of the assumptions regarding the stiffness of the gusset plates was checked indirectly by comparing theoretical and experimental buckling loads. To obtain a more direct verification a moment was applied to one joint of a plane truss and the resulting rotations of this and neighboring joints were measured. The rotations were also calculated using the stiffness and carry-over factors determined in Appendix 1 and the calculated values were compared with the test results.

The experiments were conducted with framework specimen 5 after the buckling tests of the specimen had been completed. As the stresses attained at buckling were well below the proportional limit, the buckling tests caused no permanent deformation. Stiffness tests were run first on the complete three-dimensional framework; then the braces connecting the two vertical planes were removed and the tests were repeated on the resulting two-dimensional truss. The size of the gusset plates was varied between 13.3%, 16.5%, and 20% of the length of the bars by inserting or removing some of the rivets attaching the gusset plate to the bar.

The moment was applied by an arm fitted to the upright entering the joint to be tested. Dead weights were hung from the moment arm at a point 40 in. from the joint. The loads were varied from 1 lb to 10 lb in seven or eight approximately equal increments. The specimen was thus subjected to the combined action of a shear load and a moment, but the length of the moment arm was considered sufficient to make the effect of the shear load negligible. This assumption was permissible because the resistance of the framework to forces applied centrally at the joints was very much greater than the resistance to moments that tended to rotate the joints.

To measure the rotation of a joint a short channel section was mounted with two bolts and lock nuts approximately 1 in. from the joint in question. A long channel section supported at several points was attached to the rig independently of the framework. Two dial gages were fastened to the latter channel with their plungers resting on the short channel section attached to the specimen. The difference in the gage readings divided by the distance between the gages was taken as the angle of rotation of the joint in radians.

Figs. 4 and 5 are samples of comparisons between measured and calculated values of the stiffness. The following conclusions can be drawn from these figures as well as from other graphs not shown:

(1) All the experimental points are located between the curve corresponding to infinite gusset plate rigidity and that corresponding to the hyperbolic law.

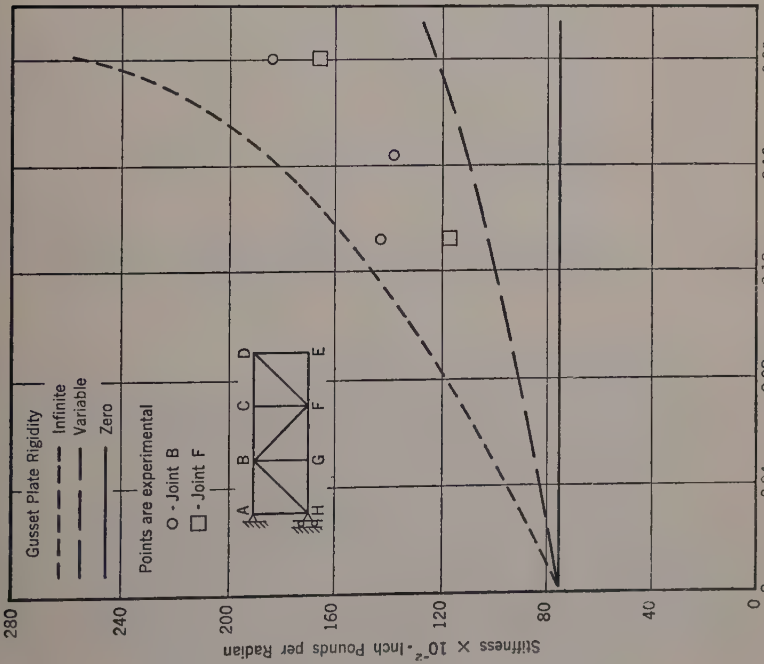

FIG. 4.—STIFFNESS OF JOINTS B AND F, SPECIMEN 5; NO AXIAL LOADS

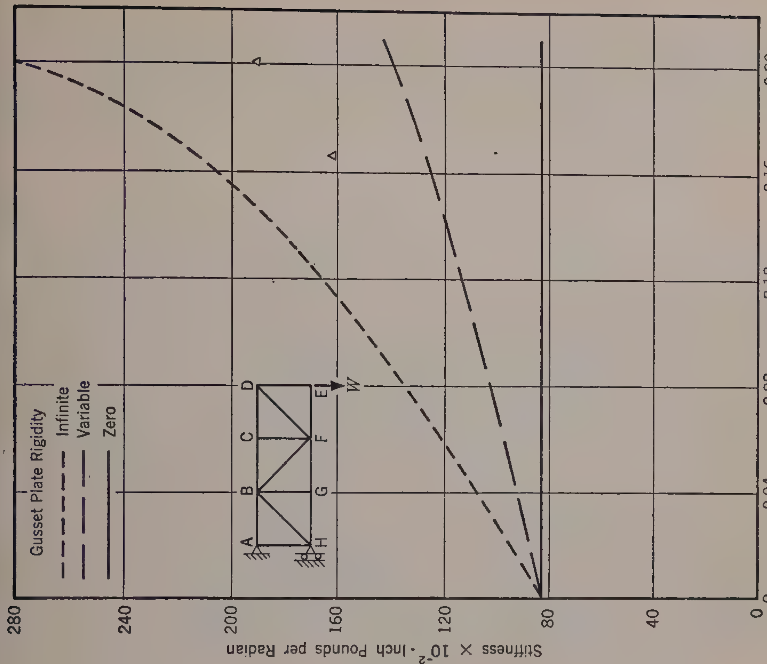

FIG. 5.—STIFFNESS OF JOINT B, SPECIMEN 5; BARS SUBJECTED TO AXIAL LOADS

(2) For small gusset plates the hyperbolic law represents a good approximation. For large gusset plates it gives a conservative estimate.

(3) The increase in stiffness due to gusset plate effect is considerable. With 20% gusset plates the actual stiffness is from two times to three times the value without gusset plates.

Conclusions

Tests on eight frameworks proved that the convergence criterion of the Hardy Cross moment distribution method can be used with confidence to predict the buckling loads of frameworks if the effect of the gusset plates on the stiffness and carry-over factors is taken into account. Values of these quantities were calculated on the basis of two different assumptions and the numerical results obtained are presented in eight graphs. It was found that the assumption of a hyperbolic law for the bending rigidity distribution yields conservative results for the buckling of trusses which are accurate enough for practical purposes when the gusset plate length divided by the total theoretical length of the truss member is not greater than 0.13. The assumption of infinite rigidity for the gusset plate regions leads to nonconservative results. The actual buckling load of a truss is bracketed by the values obtainable on the basis of these two assumptions. A numerical example is presented in Appendix 2 to show how a practical problem can be solved.

Acknowledgment

The investigations described in this paper were conducted under a contract awarded by the Office of Naval Research of the United States Navy. The writers are grateful to the Navy for permission to publish this material. They also wish to acknowledge their indebtedness to Edgar B. Beck, Bertram Klein, Bernard Levine, Harold Liebowitz, Julian Sano, Vito L. Salerno, and Hrant H. Yousoufian for their contributions to the analysis and the experimental work.

APPENDIX 1. STIFFNESS AND CARRY-OVER FACTORS FOR BARS WITH GUSSET PLATES

It has been customary to evaluate the stiffness and carry-over factors of bars on the basis of a constant bending rigidity throughout the length of the bar. When these factors were used to calculate the buckling load of the frameworks described in the experimental part of this report, the resulting theoretical buckling loads were lower than the experimental values. To eliminate this discrepancy the bending rigidity of a bar in a framework was assumed to increase hyperbolically toward the joint in the regions reinforced by gusset plates. The effect of such a variation on the stiffness of a bar with end moment, but no axial load, has been demonstrated elsewhere.[11] The theory is herein extended to bars subjected to both end moment and axial load.

As shown in Fig. 6(a), the bar is considered in three sections; the sections s and t are reinforced by gusset plates and the middle section has constant bending rigidity $E\,I$. If I is the moment of inertia of the middle section, the hyperbolic variation in the ends gives

$$I_s = \frac{s\,I}{x} \qquad (\text{for } 0 \leqq x \leqq s) \ldots\ldots (2a)$$

and

$$I_t = \frac{t\,I}{L - x} \qquad (\text{for } L - t \leqq x \leqq L) \ldots\ldots (2b)$$

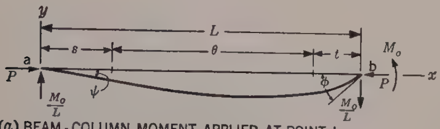

(a) BEAM-COLUMN MOMENT APPLIED AT POINT b

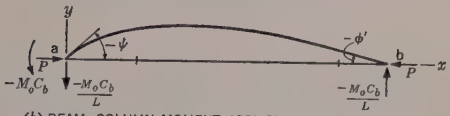

(b) BEAM-COLUMN MOMENT APPLIED AT POINT a

FIG. 6.—FORCES ON BARS WITH GUSSET PLATES

Hence, the following three moment-curvature equations can be written for the three sections if both ends of the bar are pin jointed:

$$\frac{E\,s\,I}{x}\,y''_s + P\,y_s = \frac{M_0\,x}{L} \qquad (\text{for } 0 \leqq x \leqq s) \ldots\ldots (3a)$$

$$E\,I\,y''_m + P\,y_m = \frac{M_0\,x}{L} \qquad (\text{for } s \leqq x \leqq L - t) \ldots\ldots (3b)$$

and

$$\frac{E\,I\,t}{L - x}\,y''_t + P\,y_t = \frac{M_0\,x}{L} \qquad (\text{for } L - t \leqq x \leqq L) \ldots\ldots (3c)$$

in which y'' is the second derivative of the deflection y with respect to x. The solutions to Eqs. 3 give the deflection y of the bar as

$$y_s = x^{1/2}\left[A_1\,J_{1/3}\left(\frac{2\,k\,x^{3/2}}{3\,s^{1/2}}\right) + B_1\,J_{-1/3}\left(\frac{2\,k\,x^{3/2}}{3\,s^{1/2}}\right)\right] + \alpha\,x \qquad (\text{for } 0 \leqq x \leqq s) \ldots (4a)$$

$$y_m = A_2 \sin k\,x + B_2 \cos k\,x + \alpha\,x \qquad (\text{for } s \leqq x \leqq L - t) \ldots (4b)$$

and

$$y_t = (L - x)^{1/2}\left\{A_3\,J_{1/3}\left[\frac{2\,k(L - x)^{3/2}}{3\,t^{1/2}}\right] + B_3\,J_{-1/3}\left[\frac{2\,k(L - x)^{3/2}}{3\,t^{1/2}}\right]\right\} + \alpha\,x \qquad (\text{for } L - t \leqq x \leqq L) \ldots (4c)$$

in which $k^2 = \dfrac{P}{E\,I}$, $\alpha = \dfrac{M_0}{L\,P}$, $J_{1/3}$, and $J_{-1/3}$ are Bessel functions of order 1/3 and of order $-1/3$, respectively, and A_1, A_2, A_3, B_1, B_2, and B_3 are arbitrary constants. To insure continuity of deflection and slope along the bar, the following conditions must be satisfied:

$$\left.\begin{aligned} y_s(s) &= y_m(s); \qquad & y_m(L-t) &= y_t(L-t) \\ y'_s(s) &= y'_m(s); \qquad & y'_m(L-t) &= y'_t(L-t) \end{aligned}\right\} \qquad (5)$$

Since the ends of the bar can rotate but not displace, $y(0) = y(L) = 0$. These six conditions determine the six arbitrary constants as

$$\left.\begin{aligned} A_1 &= \frac{y_1 - \alpha\, s}{s^{1/2}\, J_{1/3}(z_s)} \\ A_2 &= (y_2 - \alpha\, L + \alpha\, t)\cos k\, s - (y_1 - \alpha\, s)\cos k(L-t) \\ A_3 &= \frac{r\left[y_2 - \alpha(L-t) + \alpha\, L\left(\dfrac{k}{3}\right)^{1/3} t^{-1/6}\,\Gamma(\tfrac{2}{3})t^{1/2}\, J_{-1/3}(z_t)\right]}{t^{1/2}\, J_{1/3}(z_t)} \end{aligned}\right\} \qquad (6)$$

and

$$\left.\begin{aligned} B_1 &= 0 \\ B_2 &= -\, r\left[(y_2 - \alpha\, L + \alpha\, t)\sin k\, s + (y_1 - \alpha\, s)\sin k(L-t)\right] \\ B_3 &= -\,\alpha\, L\left(\frac{k}{3\, t^{1/2}}\right)^{1/3}\Gamma(\tfrac{2}{3}) \end{aligned}\right\} \qquad (7)$$

in which

$$y_1 - \alpha\, s = \alpha\, r\, L\left(\frac{k}{3\, t^{1/2}}\right)^{1/3}\Gamma(\tfrac{2}{3})t^{1/2}\, J_{-1/3}(z_t)\,\frac{R(z_t)}{Q(z_s)\,Q(z_t) - r^2} \qquad (8a)$$

$$y_2 - \alpha(L-t) = \alpha\, L\left(\frac{k}{3\, t^{1/2}}\right)^{1/3}\Gamma(\tfrac{2}{3})t^{1/2}\, J_{-1/3}(z_t)\,\frac{R(z_t)\,Q(z_s)}{Q(z_s)\,Q(z_t) - r^2} \qquad (8b)$$

In Eqs. 8,

$$R(z_t) = \frac{J_{2/3}(z_t)}{J_{-1/3}(z_t)} + \frac{J_{-2/3}(z_t)}{J_{1/3}(z_t)} \qquad (9a)$$

$$Q(z_t) = \frac{J_{-2/3}(z_t)}{J_{1/3}(z_t)} + \cot k\,\theta \qquad (9b)$$

$$Q(z_s) = \frac{J_{-2/3}(z_s)}{J_{1/3}(z_s)} + \cot k\,\theta \qquad (9c)$$

Also

$$r = \frac{1}{\sin k\,\theta} \qquad (10a)$$

$$z_t = \tfrac{2}{3}\, k\, t \qquad (10b)$$

$$z_s = \tfrac{2}{3}\, k\, s \qquad (10c)$$

and

$$\theta = L - s - t \qquad (10d)$$

From the foregoing solutions $y'(L)$ and $y'(0)$ are given as follows:

$$y'(L) = \alpha\,\lambda_1(s, t) \qquad (11a)$$

$$y'(0) = \alpha\,\lambda_2(s, t) \qquad (11b)$$

in which

$$\lambda_1(s, t) = 1 - \left[\frac{k\,L}{3} \left(\frac{L}{t} \right)^{1/2} \right]^{2/3} \frac{\Gamma(\frac{2}{3})}{\Gamma(\frac{4}{3})} \frac{J_{-1/3}(z_t)}{J_{1/3}(z_t)} \left[1 - \frac{R(z_t)\,Q(z_s)}{Q(z_s)\,Q(z_t) - r^2} \right] \tag{12a}$$

and

$$\lambda_2(s, t) = 1 - \left[\left(\frac{k\,L}{3} \right)^2 \left(\frac{L}{t} \right)^{1/2} \left(\frac{L}{s} \right)^{1/2} \right]^{1/3} \frac{\Gamma(\frac{2}{3})}{\Gamma(\frac{4}{3})}\, r \frac{J_{-1/3}(z_t)}{J_{1/3}(z_s)} \frac{R(z_t)}{Q(z_s)\,Q(z_t) - r^2} \tag{12b}$$

The stiffness coefficient p_b at end b of the bar in Fig. 6(a) is defined implicitly by

$$\phi = \frac{M_0\,L}{p_b\,E\,I} \tag{13a}$$

If the deflection is small, $\tan \phi \cong \phi$, and

$$y'_b(L) = \frac{M_0\,L}{p_b\,E\,I} \tag{13b}$$

Thus the stiffness coefficient at end b is

$$p_b = \frac{(k\,L)^2}{\lambda_1(s, t)} \tag{14}$$

and the carry-over factor is zero here since end a is pin jointed.

To be of use in a relaxation process such as the Hardy Cross moment distribution method, the stiffness and carry-over factors at end b of the bar must be determined with end a fixed. For this purpose a moment $(-M_0\,C_b)$ is applied at joint a (Fig. 6(b)), in which C_b is defined implicitly by the expression:

$$\psi = \frac{M_0\,C_b\,L}{p_a\,E\,I} \tag{15}$$

and p_a is the stiffness coefficient of joint a when joint b is pin jointed. Therefore,

$$C_b = \frac{\psi}{\phi} \frac{p_a}{p_b} \tag{16a}$$

If ϕ and ψ are small, the angles in Fig. 6(a) can be replaced so as to give

$$C_b = \frac{y'_b(0)}{y'_b(L)} \frac{p_a}{p_b} \tag{16b}$$

in which the subscript b in $y'_b(0)$ and $y'_b(L)$ indicates that M_0 is applied at joint b. With the notation of Fig. 6(b), the coefficient C_a is defined by the expression:

$$\phi' = \frac{M_0\,C_b\,C_a\,L}{p_b\,E\,I} = \frac{C_a\,p_a}{p_b}\,\psi \tag{17}$$

or

$$C_a = \frac{\phi'}{\psi} \frac{p_b}{p_a} \tag{18a}$$

If ϕ' and ψ are assumed to be small,

$$C_a = \frac{y'_a(0)}{y'_a(L)} \frac{p_b}{p_a} \qquad \text{(18}b\text{)}$$

in which the subscript a in $y'_a(0)$ and $y'_a(L)$ indicates that the moment is applied at joint a, and the abscissas 0 and L indicate joints b and a, respectively. This system can be derived from the system in Fig. 6(a) by interchanging s and t, since in that figure both ends are pin jointed. Thus,

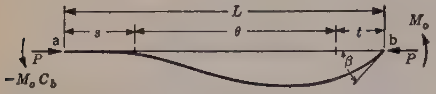

FIG. 7.—BEAM COLUMN WITH ONE END FIXED

$$y'_a(0) = \alpha\, \lambda_2(t, s) \qquad \text{and} \qquad y'_a(L) = \alpha\, \lambda_1(t, s) \qquad \text{(19}a\text{)}$$

and, consequently,

$$p_a = \frac{M_0\, L}{E\, I\, y'_a(L)} = \frac{(k\, L)^2}{\lambda_1(t, s)} \qquad \text{(19}b\text{)}$$

By superimposing the loading of Fig. 6(b) on that of Fig. 6(a), the system of Fig. 7 is obtained in which

$$\beta = \phi - \phi' = \frac{M_0\, L}{p_b\, E\, I}(1 - C_b\, C_a) = y'_b(L)\left[1 - \frac{y'_b(0)}{y'_b(L)} \frac{y'_a(0)}{y'_a(L)}\right] \qquad (20)$$

or

$$\frac{\beta}{\alpha} = \lambda_1(s, t)\left[1 - \frac{\lambda_2(s, t)\, \lambda_2(t, s)}{\lambda_1(s, t)\, \lambda_1(t, s)}\right] \qquad (21)$$

With the use of the definition expressed by Eq. 13a, the stiffness coefficient f at end b of the bar in Fig. 7 is defined by the equation:

$$\beta = \frac{M_0\, L}{f\, E\, I} \qquad (22)$$

so that

$$f = \frac{(k\, L)^2}{\dfrac{\beta}{\alpha}} \qquad (23)$$

The carry-over factor C, defined as the moment induced at joint a by a unit moment at joint b (Fig. 7), is then

$$C = C_b = \frac{y'_b(0)}{y'_b(L)} \frac{p_a}{p_b} = \frac{\lambda_2(s, t)}{\lambda_1(s, t)} \qquad (24)$$

In the case of equal gusset plates, Eqs. 20, 21, and 24 reduce to

$$\beta = y'(L)\left\{1 - \left[\frac{y'(0)}{y'(L)}\right]^2\right\} \qquad (25)$$

or

$$\frac{\beta}{\alpha} = \lambda_1(s, s)\left\{1 - \left[\frac{\lambda_2(s, s)}{\lambda_1(s, s)}\right]^2\right\} \qquad (26)$$

and

$$C = \frac{y'(0)}{y'(L)} = \frac{\lambda_2(s,\, s)}{\lambda_1(s,\, s)} \qquad \text{(27)}$$

since $p_a = p_b$, etc., due to symmetry.

The same procedure can be followed for a bar in tension with the load $(-P)$ in place of P. With this substitution, Eqs. 11 become

$$y'(L) = \alpha\, \bar{\lambda}_1(t,\, s) \qquad \text{(28}a\text{)}$$

and

$$y'(0) = \alpha\, \bar{\lambda}_2(t,\, s) \qquad \text{(28}b\text{)}$$

in which

$$\bar{\lambda}_1(t,\, s) = 1 - \left[\frac{k\,L}{3}\left(\frac{L}{t}\right)^{1/2}\right]^{2/3} \frac{\Gamma(\frac{2}{3})}{\Gamma(\frac{4}{3})}\, \frac{I_{-1/3}(z_t)}{I_{1/3}(z_t)} \left[1 - \bar{R}\, \frac{\bar{R}(z_t)\, \bar{Q}(z_s)}{\bar{Q}(z_s)\, \bar{Q}(z_t) - (\bar{r})^2}\right]. \qquad \text{(29}a\text{)}$$

and

$$\bar{\lambda}_2(t,\, s) = 1 - \left[\frac{k\,L}{3}\left(\frac{L}{t}\right)^{1/2}\right]^{1/3} \left[\frac{k\,L}{3}\left(\frac{L}{s}\right)^{1/2}\right]^{1/3} \frac{\Gamma(\frac{2}{3})}{\Gamma(\frac{4}{3})}$$

$$\times \left(\frac{\frac{t}{L}}{\frac{s}{L}}\right)^{1/2} \frac{I_{-1/3}(z_t)}{I_{1/3}(z_s)}\, \bar{r}\, \frac{\bar{R}(z_t)}{\bar{Q}(z_t)\, \bar{Q}(z_s) - (\bar{r})^2} \qquad \text{(29}b\text{)}$$

Also,

$$\bar{R}(z_t) = \frac{I_{-2/3}(z_t)}{I_{1/3}(z_t)} - \frac{I_{2/3}(z_t)}{I_{-1/3}(z_t)} \qquad \text{(30}a\text{)}$$

$$\bar{Q}(z_t) = \frac{I_{-2/3}(z_t)}{I_{1/3}(z_t)} + \coth k\,\theta \qquad \text{(30}b\text{)}$$

$$\bar{Q}(z_s) = \frac{I_{-2/3}(z_s)}{I_{1/3}(z_s)} + \coth k\,\theta \qquad \text{(30}c\text{)}$$

$$z_t = \tfrac{2}{3}\,k\,t \qquad \text{(30}d\text{)}$$

$$z_s = \tfrac{2}{3}\,k\,s \qquad \text{(30}e\text{)}$$

$$\bar{r} = \frac{1}{\sinh k\,\theta} \qquad \text{(30}f\text{)}$$

and

$$\theta = L - s - t \qquad \text{(30}g\text{)}$$

In Eqs. 29 and 30, I is the usual notation for the modified Bessel function.

Calculations have been made and curves of stiffness and carry-over factors drawn for bars of equal gusset plates occupying 9%, 13.3%, 20%, and 30% of the length of the bar. The curves are presented in Figs. 8 and 9.

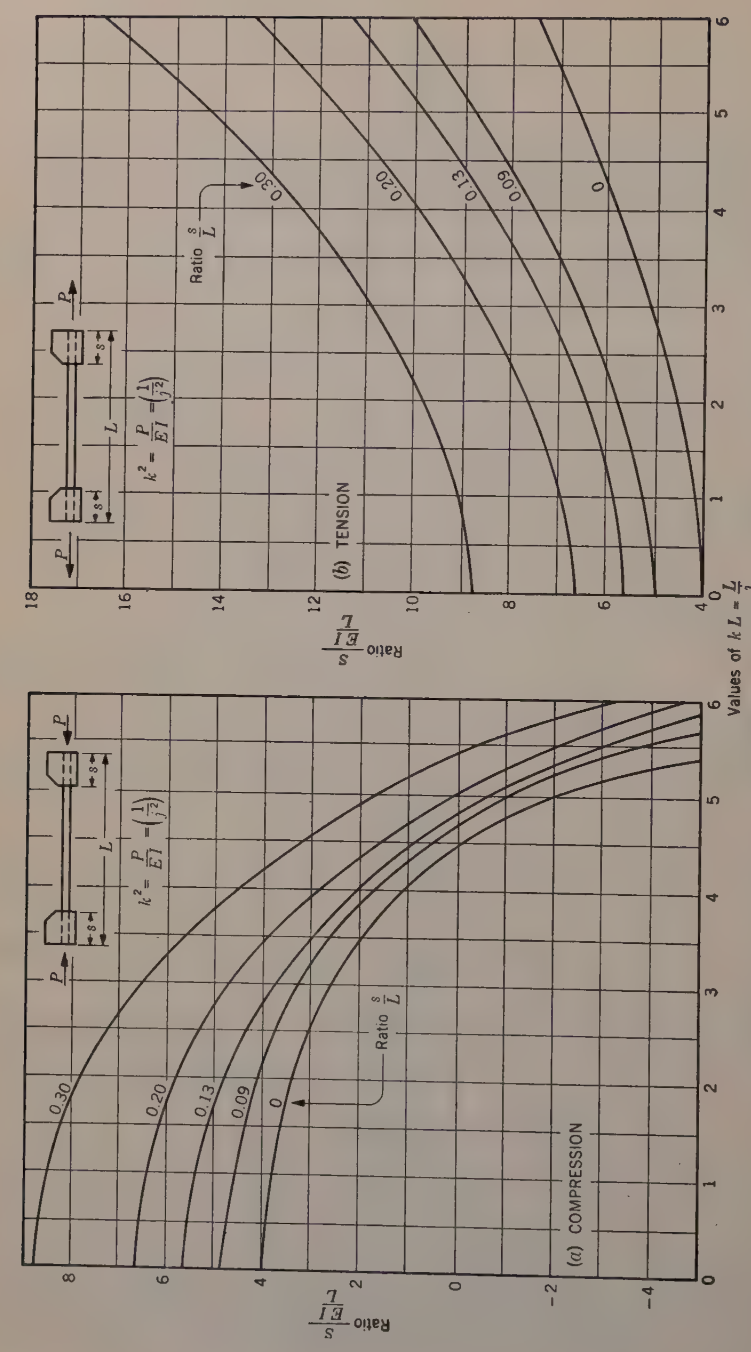

FIG. 8.—STIFFNESS FACTORS FOR BARS WITH GUSSET PLATES; VARIABLE GUSSET PLATE RIGIDITY

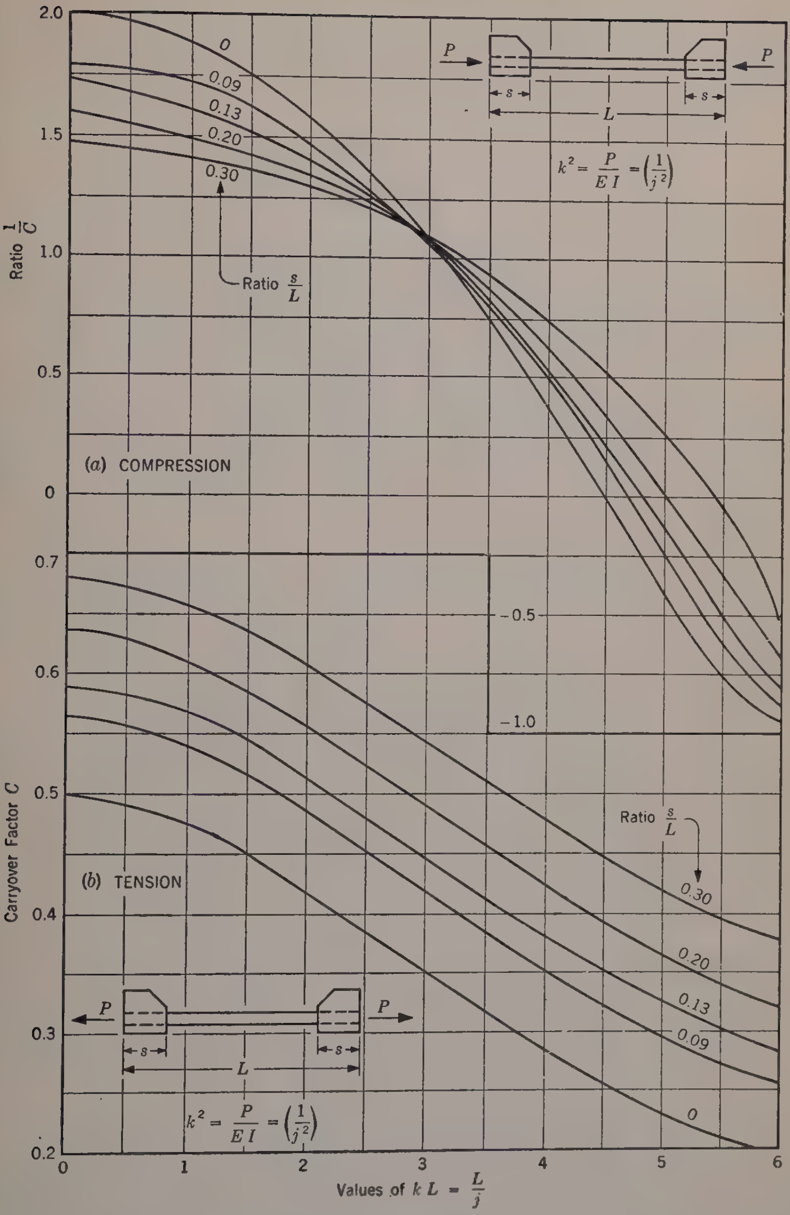

FIG. 9.—CARRY-OVER FACTORS FOR BARS WITH GUSSET PLATES; VARIABLE GUSSET PLATE RIGIDITY

For purposes of comparison it is of interest to calculate stiffness and carry-over factors based on the assumption of infinitely rigid gusset plates. The differential equations of bending, for the bar in Fig. 6(a), when the infinite moment of inertia extends over regions of lengths s and t at the left and right ends of the bar, respectively, are

$$y''_s = 0 \qquad (\text{for } 0 \leqq x \leqq s) \tag{31a}$$

$$E\,I\,y''_m + P\,y_m = \frac{M_0\,x}{L} \qquad (\text{for } s \leqq x \leqq L - t) \tag{31b}$$

and

$$y''_t = 0 \qquad (\text{for } L - t \leqq x \leqq L) \tag{31c}$$

in which y'' is the second derivative of the deflection y with respect to x. The solutions to these equations give the deflection y of the bar as

$$y_s = A_1\,x + B_1 \qquad (\text{for } 0 \leqq x \leqq s) \tag{32a}$$

$$y_m = A_2 \sin k\,x + B_2 \cos k\,x + \alpha\,x \qquad (\text{for } s \leqq x \leqq L - t) \tag{32b}$$

and

$$y_t = A_3\,x + B_3 \qquad (\text{for } L - t \leqq x \leqq L) \tag{32c}$$

in which $k^2 = \dfrac{P}{E\,I}$, $\alpha = \dfrac{M_0}{L\,P}$, and A_1, A_2, A_3, B_1, B_2, and B_3 are arbitrary constants. The same conditions on the deflection y and the slope y' as given in the preceding calculations may be used to determine these six arbitrary constants. The result is

$$\left.\begin{aligned} A_1 &= y'(0) = \alpha - \frac{\alpha\,k\,L}{(1 - k^2\,s\,t)\sin k\,\theta + k(t + s)\cos k\,\theta} \\ A_2 &= \frac{1}{k \sin k\,\theta}\left[(A_1 - \alpha)\sin k(L - t) - (A_3 - \alpha)\sin k\,s\right] \\ A_3 &= y'(L) = \alpha - (\alpha\,k\,L)\frac{\cos k\,\theta - k\,s \sin k\,\theta}{(1 - k^2\,s\,t)\sin k\,\theta + k(t + s)\cos k\,\theta} \end{aligned}\right\} \tag{33}$$

and

$$\left.\begin{aligned} B_1 &= 0 \\ B_2 &= \frac{1}{k \sin k\,\theta}\left[(A_1 - \alpha)\cos k(L - t) - (A_3 - \alpha)\cos k\,s\right] \\ B_3 &= -A_3\,L \end{aligned}\right\} \tag{34}$$

in which

$$\theta = L - s - t \tag{35}$$

A procedure entirely analogous to that employed for the calculation of stiffness and carry-over factors under the assumption of a hyperbolic variation of the moment of inertia in the regions of the bar reinforced by gusset plates leads, in this case, to the following expressions for the stiffness factor S and the carry-over factor C for a bar whose far end is fixed:

$$S = \frac{E\,I}{L}(k\,L)^2\frac{\alpha}{\beta} \tag{36a}$$

and

$$C = \frac{A_1}{\lambda(s, t)} \quad (36b)$$

in which

$$\beta = \lambda(s, t)\left[1 - \frac{A^2_1}{\lambda(s, t)\,\lambda(t, s)}\right] \quad (37)$$

For the case of a bar in compression,

$$\lambda(s, t) = A_3 \quad (38)$$

whereas, for a bar in tension,

$$\lambda(s, t) = \alpha - (\alpha\, k\, L)\frac{\cosh k\,\theta + k\, s \sinh k\,\theta}{(1 - k^2\, s\, t)\sinh k\,\theta + k(t + s)\cosh k\,\theta} \quad (39)$$

Numerical values of the stiffness and carry-over factors have been calculated for gusset plates of equal length at the two ends of the bar extending over 9%, 13.3%, and 20% of the length of the bar. The values are plotted in Figs. 10 and 11.

APPENDIX 2. NUMERICAL EXAMPLE

The buckling load will be calculated here for specimen 4 whose configuration and dimensions are given in Fig. 3(*c*). The gusset plates extend over 9% of the length of the members. The material used in the construction of the framework is 24S-T aluminum alloy. The first step is the assumption of a value for the load applied to the structure. In this case the load W was chosen as 100 lb acting at the end of the loading frame previously described, which corresponds to an applied bending moment of 6,000 in-lb, and an applied shear force of 100 lb at the loaded end of the structure. This assumption leads to the forces given in Cols. 3 and 4, Table 2(*a*). The entries in Cols. 5 and 6 are calculated from the forces and the geometric and mechanical properties of the bar. The reciprocal of the carry-over factor is given for the compression bars in Col. 7 as read from the curves of Fig. 9(*a*). The values in Col. 8 are found from Fig. 8(*a*) for the compression members and from Fig. 8(*b*) for the tension members. The stiffness factors of Col. 10 are easily obtained from the values in Cols. 1 and 2. The corresponding distribution factors are given in Fig. 12(*a*).

Since the values of $k\,L\left(= \frac{L}{j}\right)$ are smaller than $2\,\pi$ for all the compression members, and greater than π for some of them, and because the sums ΣS of the stiffnesses are positive at every joint, the stability must be determined by the convergence criterion. First, a moment of 1,000 in-lb is applied at joint J. The joint is balanced, and moments are carried over to the adjacent joints. The balancing procedure, shown in Fig. 12(*a*), is then continued in a straightforward manner, except that carry-over moments are accumulated at joint J and are never balanced out. When all the joints but J are balanced, the total accumulated moments at J are added. In this case, the sum is found to be a

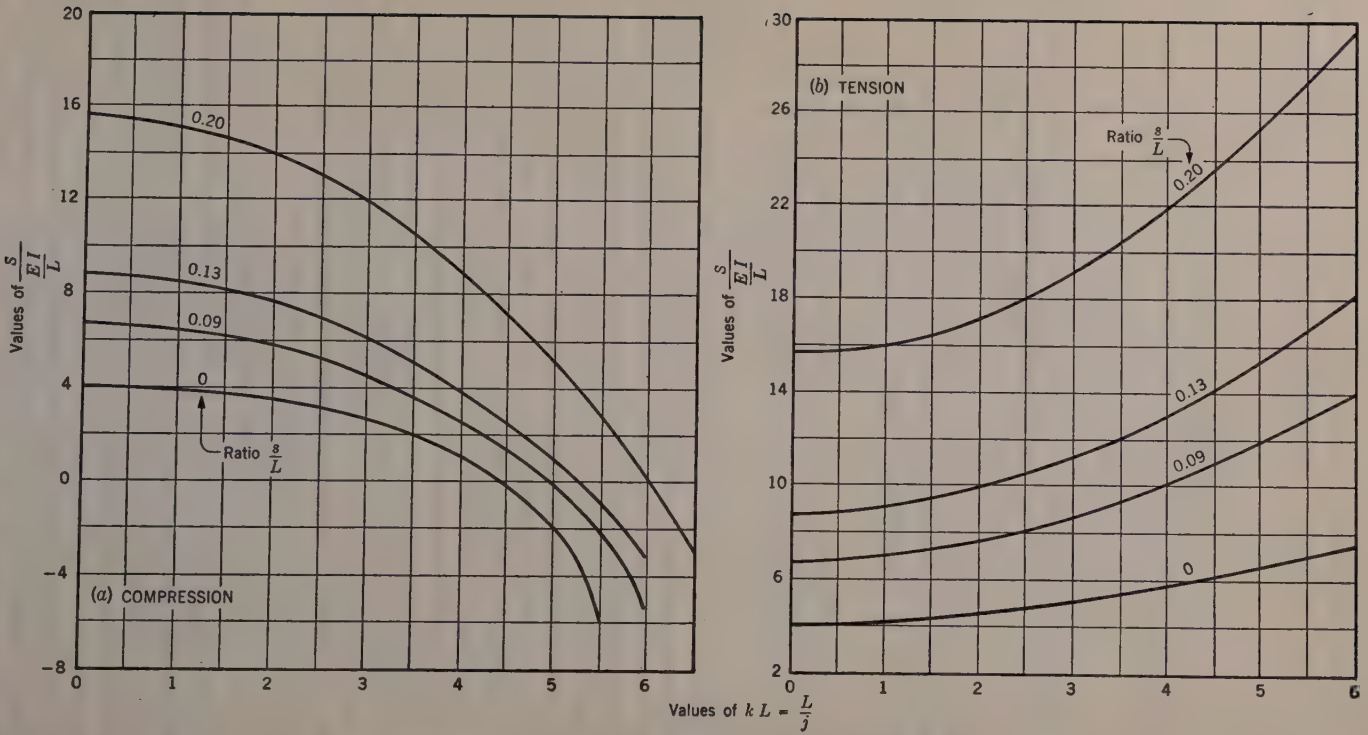

FIG. 10.—STIFFNESS FACTORS FOR BARS WITH GUSSET PLATES; INFINITE GUSSET PLATE RIGIDITY

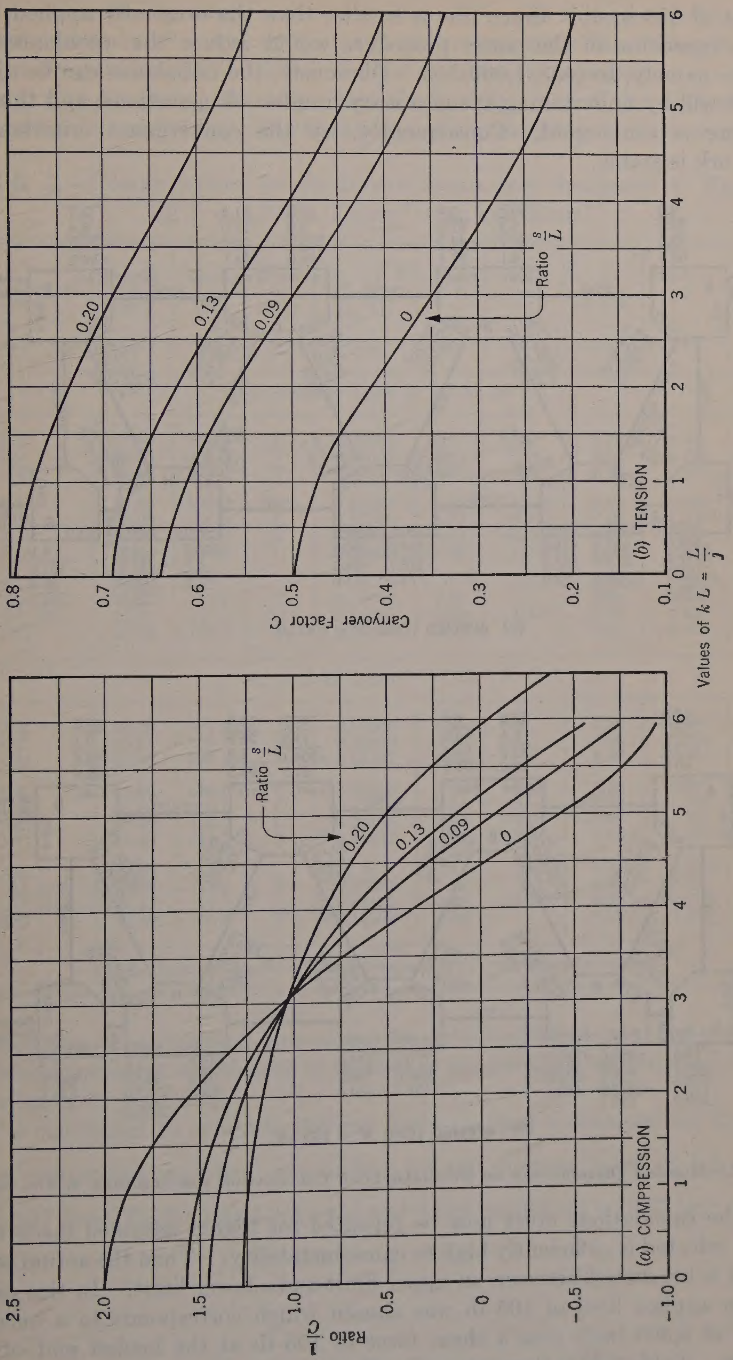

FIG. 11.—CARRY-OVER FACTORS FOR BARS WITH GUSSET PLATES; INFINITE GUSSET PLATE RIGIDITY

moment of 553 in.-lb. Since this is smaller than the originally applied 1,000 in-lb, a repetition of the entire procedure would reduce the unbalance at J further—namely, to (553/1,000)553. Obviously, the unbalance can be diminished at will by undertaking the necessary number of operations, and thus the procedure is convergent. Consequently, by the convergence criterion the framework is stable.

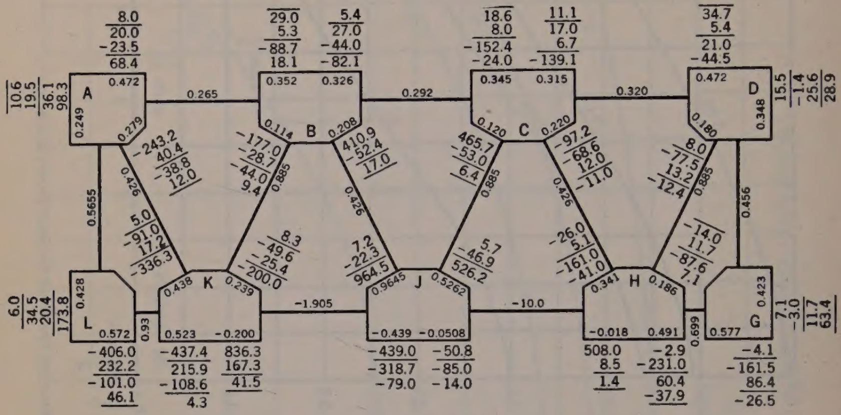

(*a*) APPLIED LOAD W = 100 LB

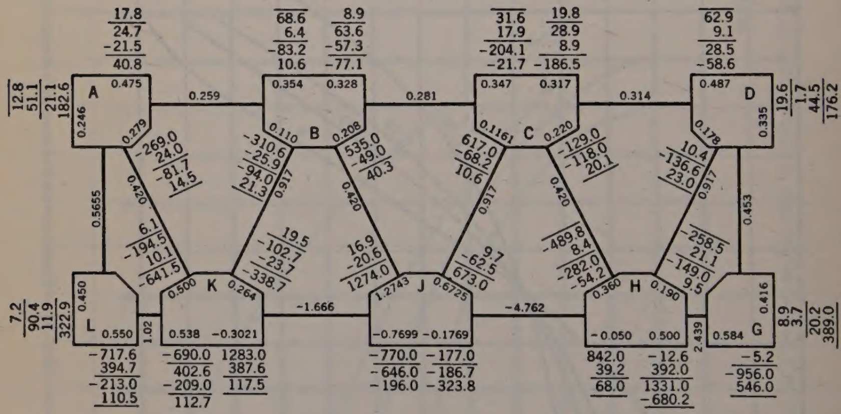

(*b*) APPLIED LOAD W = 105 LB

FIG. 12.—MOMENT DISTRIBUTION OF BUCKLING LOAD CALCULATION FOR SPECIMEN 4, FIG. 3(*c*)

All the calculations must now be repeated for higher assumed loads until the load selected is sufficiently high to cause instability. Then the actual buckling load is bracketed between an upper limit and a lower limit. In this calculation an applied load of 105 lb was chosen which corresponds to a bending moment of 6,300 in-lb plus a shear force of 105 lb at the loaded end of the structure. Table 2(*b*) is then set up like Table 2(*a*). The balancing procedure, similar to that in Fig. 12(*a*) is shown in Fig. 12(*b*). In this case the moments accumulated at joint J add up to 1,409 in-lb; and, since this value is larger than the originally applied 1,000 in-lb, the structure is unstable.

It may be concluded, therefore, that the buckling load of this framework is between 100 lb and 105 lb. The buckling load can be obtained more accurately by repeating the foregoing procedure for intermediate loads, but for most practical purposes it is sufficient to state that the buckling load is 102.5 lb with a possible error of ±2.5%.

TABLE 2.—COMPUTATION OF BUCKLING LOAD FOR SPECIMEN 4, FIG. 3(*c*) (EI = 6,835.5 LB-IN.^{2} FOR ALL BARS)

Bar (see Fig. 1) (1)	Length, L (in.) (2)	Load, P (lb) (3)	Type of load[a] (4)	$k = \sqrt{\frac{P}{EI}}$ (in.$^{-1}$) (5)	kL (6)	$\frac{1}{C}$[b] (7)	$\frac{S}{EI/L}$ (8)	C (9)	$\frac{20\,S}{EI}$ (10)
(*a*) APPLIED LOAD W = 100 LB									
AB	20.00	550.0	T	0.28366	5.67	....	9.63	0.265	9.63
BC	20.00	450.0	T	0.25658	5.13	....	8.92	0.292	8.92
CD	20.00	350.0	T	0.22628	4.53	....	8.15	0.320	8.15
LK	10.00	600.0	C	0.29627	2.96	1.075	3.40	0.930	6.80
KJ	20.00	500.0	C	0.27046	5.41	−0.525	−2.60	−1.905	−2.60
JH	20.00	400.0	C	0.24191	4.84	−0.100	−0.30	−10.0	−0.30
HG	10.00	300.0	C	0.20950	2.09	1.430	4.10	0.699	8.20
AL	20.00	0	....	0	0	....	5.078	0.5655	5.078
AK, BJ, CH	22.37	111.9	T	0.12795	2.86	....	6.38	0.426	5.70
KB, JC, HD	22.37	111.9	C	0.12795	2.86	1.130	3.48	0.885	3.11
DG	20.00	100.0	T	0.12095	2.42	....	6.02	0.456	6.02
(*b*) APPLIED LOAD W = 105 LB									
AB	20.00	577.5	T	0.29066	5.81	....	9.82	0.259	9.82
BC	20.00	472.5	T	0.26292	5.26	....	9.08	0.281	9.08
CD	20.00	367.5	T	0.23187	4.64	....	8.30	0.314	8.30
LK	10.00	630.0	C	0.31489	3.15	0.98	3.10	1.020	6.20
KJ	20.00	525.0	C	0.27714	5.54	−0.60	−3.48	−1.666	−3.48
JH	20.00	420.0	C	0.24788	4.96	−0.21	−0.80	−4.762	−0.80
HG	10.00	315.0	C	0.21467	2.15	0.41	4.00	2.439	8.00
AL	20.00	0	....	0	0	....	5.078	0.5655	5.078
AK, BJ, CH	22.37	117.5	T	0.13111	2.93	....	6.44	0.420	5.76
KB, JC, HD	22.37	117.5	C	0.13111	2.93	1.09	3.40	0.917	3.04
KG	20.00	105.0	T	0.12394	2.48	....	5.70	0.453	5.70

[a] T = "tension" and C = "compression." [b] Compression bars only.

It is of interest to compute the end fixity coefficient obtained for the most highly compressed member. As in bar KJ the average value of $kL = \frac{L}{j}$ is about 5.47 from Tables 1 and 2(*a*); the end fixity coefficient is $(5.47/\pi)^2 = 3.02$.